

On the explicit two-stage fourth-order accurate time discretizations

Yuhuan Yuan, Huazhong Tang*

Center for Applied Physics and Technology, HEDPS, and LMAM, School of Mathematical Sciences, Peking University, Beijing 100871, P.R. China

Abstract

This paper continues to study the explicit two-stage fourth-order accurate time discretizations [5, 7]. By introducing variable weights, we propose a class of more general explicit one-step two-stage time discretizations, which are different from the existing methods, such as the Euler methods, Runge-Kutta methods, and multistage multiderivative methods etc. We study the absolute stability, the stability interval, and the intersection between the imaginary axis and the absolute stability region. Our results show that our two-stage time discretizations can be fourth-order accurate conditionally, the absolute stability region of the proposed methods with some special choices of the variable weights can be larger than that of the classical explicit fourth- or fifth-order Runge-Kutta method, and the interval of absolute stability can be almost twice as much as the latter. Several numerical experiments are carried out to demonstrate the performance and accuracy as well as the stability of our proposed methods.

Keywords: Multistage multiderivative methods, Runge-Kutta methods, absolute stability region, interval of absolute stability.

1. Introduction

The explicit two-stage fourth-order accurate time discretizations are studied in [5, 7] and successfully applied to the nonlinear hyperbolic conservation laws. They belong to the two-derivative Runge-Kutta methods, see [3, 1, 6]. In comparison with the explicit four-stage fourth-order accurate Runge-Kutta method, they only call the time-consuming exact or approximate Riemann solver and the initial reconstruction with the characteristic decomposition twice at each time step, which is half of the former.

*Corresponding author. Fax: +86-10-62751801.

Email addresses: 1548602562@qq.com (Yuhuan Yuan), hztang@math.pku.edu.cn (Huazhong Tang)

For the sake of simplicity, let us consider the initial-value problem of the first-order ordinary differential equation (ODE)

$$u'(t) = L(t, u), \quad t \in [0, T]; \quad u(0) = u_0, \quad (1.1)$$

where u is scalar and $L(t, u)$ is linear or nonlinear with respect to u . Assume that the solution u of (1.1) is a sufficiently smooth function of t and L is also smooth, and give a partition of the time interval by $t_{n+1} = t_n + \tau$, $n \in \mathbb{Z}^+ \cup \{0\}$, where τ denotes the time step-size. The Taylor series expansion of u in t reads

$$\begin{aligned} u^{n+1} &= \left(u + \tau u_t + \frac{\tau^2}{2!} u_{tt} + \frac{\tau^3}{3!} u_{ttt} + \frac{\tau^4}{4!} u_{tttt} \right)^n + \mathcal{O}(\tau^5) \\ &= \left(u + \tau L(t, u) + \frac{\alpha \tau^2}{2} \mathcal{D}_t L(t, u) \right)^n \\ &\quad + \frac{(1-\alpha)\tau^2}{2} \left(\left(u + \frac{\tau}{3(1-\alpha)} L(t, u) + \frac{\tau^2}{12(1-\alpha)} \mathcal{D}_t L(t, u) \right)_{tt} \right)^n + \mathcal{O}(\tau^5), \end{aligned} \quad (1.2)$$

where $\mathcal{D}_t = \partial_t + L\partial_u$ and α does not depend on t, u .

Based on the additive decomposition (1.2) with $\alpha = 1/3$, the explicit two-stage fourth-order time-accurate discretization [5] can be implemented as follows

$$\begin{aligned} u^* &= u^n + \frac{\tau}{2} L(t^n, u^n) + \frac{\tau^2}{8} (\mathcal{D}_t L)(t^n, u^n), \\ u^{n+1} &= u^n + \tau L(t^n, u^n) + \frac{\tau^2}{6} \left[(\mathcal{D}_t L)(t^n, u^n) + 2(\mathcal{D}_t L)(t^n + \tau/2, u^*) \right], \end{aligned} \quad (1.3)$$

which can also be found in [3, Section 3], [1, Section 3.2] and [6, Section 1]. For a general choice of α that $\alpha = \alpha(\hat{\tau})$ is a differentiable function of $\hat{\tau} = \tau^p$, $p \geq 1$, and satisfies $\alpha = 1/3 + \mathcal{O}(\hat{\tau})$ and $\alpha \neq 1$, the general two-stage fourth-order time-accurate discretization [7] can be given as follows

$$\begin{aligned} u^* &= u^n + \frac{\tau}{3(1-\alpha)} L(t^n, u^n) + \frac{\tau^2}{12(1-\alpha)} (\mathcal{D}_t L)(t^n, u^n), \\ u^{n+1} &= u^n + \tau L(t^n, u^n) + \frac{\tau^2}{2} \left[\alpha (\mathcal{D}_t L)(t^n, u^n) + (1-\alpha) (\mathcal{D}_t L) \left(t^n + \frac{\tau}{3(1-\alpha)}, u^* \right) \right], \end{aligned} \quad (1.4)$$

which are not mentioned in the literature. It's easy to verify that the stability polynomials for both two-stage schemes (1.3) and (1.4) are

$$\pi(\theta, z) = \theta - \left(1 + z + \frac{1}{2}z^2 + \frac{1}{6}z^3 + \frac{1}{24}z^4 \right),$$

which is the same as that of the (classical) explicit four-stage fourth-order accurate Runge-Kutta method. For the absolute stability [2, 4], one requires that

$$\left| 1 + z + \frac{1}{2}z^2 + \frac{1}{6}z^3 + \frac{1}{24}z^4 \right| \leq 1.$$

It is worth noting that there exist some examples of inequivalent definitions of the region of absolute stability of a numerical method for ODEs in the literature¹.

Does there exist any explicit two-stage fourth-order accurate time discretization with a larger region of absolute stability? The aim of this paper is to answer this question and to propose a class of new and more general explicit one-step two-stage time discretizations with variable weights, which depend on the time step-size and the dependent and independent variables. It should be emphasized that those new time discretizations can have larger absolute stability regions and intervals than the classical explicit fourth- or fifth-order Runge-Kutta method, when the variable weights are specially chosen.

The paper is organized as follows. Section 2 proposes the general two-stage fourth-order methods. Section 3 discusses the absolute stability of the proposed methods. Section 4 conducts several numerical experiments to demonstrate the performance and accuracy as well as the stability of the proposed methods. Conclusions are given in Section 5.

2. Numerical methods

This section proposes a class of new and more general explicit one-step two-stage time discretizations.

Instead of the additive decomposition in (1.2), let us consider a more general decomposition

$$u^{n+1} = \left(u + \tau L(t, u) + \frac{\alpha\tau^2}{2} \mathcal{D}_t L(t, u) \right)^n + \frac{\beta\tau^2}{2} \left(\left(u + \frac{\tau}{3\beta} L(t, u) + \frac{\tau^2}{12\beta} \mathcal{D}_t L(t, u) \right)_{tt} \right)^n + \mathcal{O}(\tau^5), \quad (2.1)$$

where $\alpha = \alpha(t^n, u^n, \tau)$ and $\beta = \beta(t^n, u^n, \tau)$ are two variable weights, depending on the time step-size and the dependent and independent variables. Based on (2.1), the new and explicit

¹ <http://vmm.math.uci.edu/ODEandCM/StabilityRegionDefinitions/StabilityRegionDefinitions.html>

two-stage time discretization can be given as follows

$$\begin{aligned} u^* &= u^n + \frac{\tau}{3\beta(t^n, u^n, \tau)} L(t^n, u^n) + \frac{\tau^2}{12\beta(t^n, u^n, \tau)} (\mathcal{D}_t L)(t^n, u^n), \\ u^{n+1} &= u^n + \tau L(t^n, u^n) + \frac{\tau^2}{2} [\alpha(t^n, u^n, \tau) (\mathcal{D}_t L)(t^n, u^n) + \beta(t^n, u^n, \tau) (\mathcal{D}_t L)(t^*, u^*)], \end{aligned} \quad (2.2)$$

where

$$t^* = t^n + \frac{\tau}{3\beta(t^n, u^n, \tau)}.$$

The following theorem gives the accuracy of the new scheme (2.2) in the sense of truncation error.

Theorem 2.1. *If the variable weights $\alpha(t, u, \tau)$ and $\beta(t, u, \tau)$ satisfy*

$$\alpha(t^n, u^n, \tau) + \beta(t^n, u^n, \tau) = 1 + \mathcal{O}(\tau^3), \quad \beta(t^n, u^n, \tau) = \frac{2}{3} + \mathcal{O}(\tau), \quad (2.3)$$

then the two-stage time discretizations (2.2) are of fourth-order accuracy in the sense of truncation error, i.e.,

$$u^{n+1} = \left(u + \tau u_t + \frac{\tau^2}{2!} u_{tt} + \frac{\tau^3}{3!} u_{ttt} + \frac{\tau^4}{4!} u_{tttt} \right)^n + \mathcal{O}(\tau^5).$$

Proof For the sake of brevity, we omit all superscripts n , write $L(t^n, u^n)$ as L , and use the subscript u (resp. t) to stand for the partial derivative with respect to u (resp. t), for example, L_t and L_{uu} stand for $\frac{\partial L}{\partial t}(t^n, u^n)$ and $\frac{\partial^2 L}{\partial u^2}(t^n, u^n)$, respectively, etc. The Taylor series expansion of $(\mathcal{D}_t L)\left(t + \frac{\tau}{3\beta}, u^*\right)$ at (t, u) reads

$$\begin{aligned} (\mathcal{D}_t L)\left(t + \frac{\tau}{3\beta}, u^*\right) &= (\mathcal{D}_t L) + \frac{\tau}{3\beta} (\mathcal{D}_t L)_t + (u^* - u) (\mathcal{D}_t L)_u \\ &+ \frac{1}{2} \left(\frac{\tau^2}{9\beta^2} (\mathcal{D}_t L)_{tt} + 2(u^* - u) \frac{\tau}{3\beta} (\mathcal{D}_t L)_{ut} + (u^* - u)^2 (\mathcal{D}_t L)_{uu} \right) + \dots \end{aligned}$$

The hypothesis (2.3) implies

$$\frac{\tau}{3\beta} = \mathcal{O}(\tau), \quad (u^* - u) = \frac{\tau}{3\beta} \left(L + \frac{\tau}{4} \mathcal{D}_t L \right) = \mathcal{O}(\tau).$$

Thus, one has

$$\begin{aligned} (\mathcal{D}_t L)\left(t + \frac{\tau}{3\beta}, u^*\right) &= (\mathcal{D}_t L) + \frac{\tau}{3\beta} (\mathcal{D}_t L)_t + \frac{\tau}{3\beta} \left(L + \frac{\tau}{4} \mathcal{D}_t L \right) (\mathcal{D}_t L)_u \\ &+ \frac{\tau^2}{18\beta^2} (\mathcal{D}_t L)_{uu} L^2 + \frac{\tau^2}{9\beta^2} (\mathcal{D}_t L)_{ut} L + \frac{\tau^2}{18\beta^2} (\mathcal{D}_t L)_{tt} + \mathcal{O}(\tau^3). \end{aligned}$$

Substituting it into (2.1) gives

$$u^{n+1} = u + \tau L + \frac{\tau^2}{2}(\alpha + \beta)\mathcal{D}_t L + \frac{\tau^3}{6} \{(\mathcal{D}_t L)_t + (\mathcal{D}_t L)_u L\} \\ + \frac{\tau^4}{24} \left\{ (\mathcal{D}_t L)_u \cdot (\mathcal{D}_t L) + \frac{3}{2\beta} [(\mathcal{D}_t L)_{uu} L^2 + 2(\mathcal{D}_t L)_{ut} L + (\mathcal{D}_t L)_{tt}] \right\} + \mathcal{O}(\tau^5). \quad (2.4)$$

On the other hand, some manipulations can give

$$\begin{cases} \mathcal{D}_t L = L_u L + L_t, & (\mathcal{D}_t L)_u = L_{uu} L + L_{ut} + (L_u)^2, & (\mathcal{D}_t L)_t = L_{ut} L + L_{tt} + L_u L_t, \\ (\mathcal{D}_t L)_{uu} = L_{uuu} L + L_{uut} + 3L_{uu} L_u, & (\mathcal{D}_t L)_{ut} = L_{uut} L + L_{utt} + L_{uu} L_t + 2L_{ut} L_u, \\ (\mathcal{D}_t L)_{tt} = L_{utt} L + L_{ttt} + 2L_{ut} L_t + L_{tt} L_u, \end{cases}$$

and

$$\begin{cases} \mathcal{D}_t^2 L = [L_{uu} L^2 + 2L_{ut} L + L_{tt}] + [(L_u)^2 L + L_u L_t], \\ \mathcal{D}_t^3 L = [L_{uuu} L^3 + 3L_{uut} L^2 + 3L_{utt} L + L_{ttt}] + [(L_u)^3 L + (L_u)^2 L_t] \\ \quad + [3L_{uu} L_u L + 3L_{uu} L_t L + 3L_{ut} L_u L + 3L_{ut} L_t] + [L_{uu} L_u L^2 + 2L_{ut} L_u L + L_{tt} L_u]. \end{cases}$$

Thus, one obtains

$$\begin{cases} \mathcal{D}_t^2 L = (\mathcal{D}_t L)_t + (\mathcal{D}_t L)_u L, \\ \mathcal{D}_t^3 L = (\mathcal{D}_t L)_{uu} L^2 + 3(\mathcal{D}_t L)_{ut} L + (\mathcal{D}_t L)_{tt} + (\mathcal{D}_t L)_u \cdot (\mathcal{D}_t L). \end{cases}$$

Combining it with (2.4) yields

$$u^{n+1} = u + \tau L + \frac{\tau^2}{2}\mathcal{D}_t L + \frac{\tau^3}{6}\mathcal{D}_t^2 L + \frac{\tau^4}{24}\mathcal{D}_t^3 L \\ + \frac{\tau^2}{2}(1 - \alpha - \beta)\mathcal{D}_t L + \frac{\tau^4}{24} \left(1 - \frac{3}{2\beta}\right) \cdot [(\mathcal{D}_t L)_{uu} L^2 + 2(\mathcal{D}_t L)_{ut} L + (\mathcal{D}_t L)_{tt}] + \mathcal{O}(\tau^5).$$

Hence, if $\alpha(t, u, \tau)$, $\beta(t, u, \tau)$ satisfy (2.3), then the explicit two-stage time discretization (2.2) is fourth-order accurate. \square

Remark 2.1. If $\alpha = \frac{1}{3}$ and $\beta = \frac{2}{3}$, then (2.2) becomes the two-stage fourth-order time discretizations (1.3) proposed in [5]. If $\beta = 1 - \alpha$ and $\alpha = \alpha(\hat{\tau})$ is a differentiable function of $\hat{\tau} = \tau^p$, ($p \geq 1$) and satisfies $\alpha = 1/3 + \mathcal{O}(\hat{\tau})$, $\alpha \neq 1$, then (2.2) becomes (1.4) studied in [7]. Obviously, those special constant weights satisfy the condition (2.3).

3. Absolute stability analysis

This section discusses the absolute stability of the general two-stage fourth-order time discretizations (2.2), and gives some good choices of the variable weights α and β . Under the hypothesis (2.3), our attention will be paid to the case of that

$$\alpha + \beta = 1 + \frac{C}{60} (\tau L_u(t^n, u^n))^3, \quad (3.1)$$

where C is constant.

Consider the model problem

$$u'(t) = \lambda u(t), \quad u(0) = u_0, \quad (3.2)$$

with $\text{Re}(\lambda) \leq 0$. Applying the general two-stage fourth-order methods (2.2) to the model problem (3.2) with $L(t, u) = \lambda u(t)$ gives

$$u^{n+1} = u^n + z u^n + \frac{\alpha + \beta}{2} z^2 u^n + \frac{1}{6} z^3 u^n + \frac{1}{24} z^4 u^n,$$

where $z := \tau \lambda$. Combining it with (3.1) gives the (absolute) stability region

$$R_A(C) := \{z \in \mathbb{C} : |f(z, C)| \leq 1, \text{Re}(z) \leq 0\},$$

and the stability interval

$$I(C) := \{z \in \mathbb{R} : -1 \leq f(z, C) \leq 1, z \leq 0\},$$

where the increment function (or stability function) is defined by

$$f(z, C) = 1 + z + \frac{1}{2} z^2 + \frac{1}{6} z^3 + \frac{1}{24} z^4 + \frac{C}{120} z^5. \quad (3.3)$$

It is seen that the absolute stability region $R_A(C)$ of (2.2) is the same as that of the classical explicit fourth- and fifth-order Runge-Kutta methods when $C = 0$ and 1, respectively, and for the model problem (3.2), the two-stage fourth-order time discretizations (2.2) with (2.3) and (3.1) is fifth-order accurate in the sense of truncation error if $C = 1$.

Figures 3.1-3.3 plot the sets of complex numbers z such that $|f(z, C)| = 1$, which are also showing the loci of the boundary of the absolute stability regions R_A of the general two-stage fourth-order time discretizations (2.2) with different C . The results show that

$$\begin{cases} R_A(-2) \subsetneq R_A(-1) \subsetneq R_A(-\frac{1}{2}) \subsetneq R_A(0), \\ I(-2) \subsetneq I(-1) \subsetneq I(-\frac{1}{2}) \subsetneq I(0), \end{cases}$$

$$\begin{cases} R_A(0) \subsetneq R_A(\frac{2}{5}), R_A(0) \subsetneq R_A(\frac{1}{2}), R_A(0) \subsetneq R_A(\frac{5}{6}), \\ I(0) \subsetneq I(1), I(1) \subsetneq I(\frac{2}{5}), I(1) \subsetneq I(\frac{5}{6}) \subsetneq I(\frac{1}{2}), \\ R_A(1) \supsetneq R_A(\frac{6}{5}) \supsetneq R_A(\frac{5}{4}) \supsetneq R_A(2), \\ I(1) \supsetneq I(\frac{6}{5}) \supsetneq I(\frac{5}{4}) \supsetneq I(2). \end{cases}$$

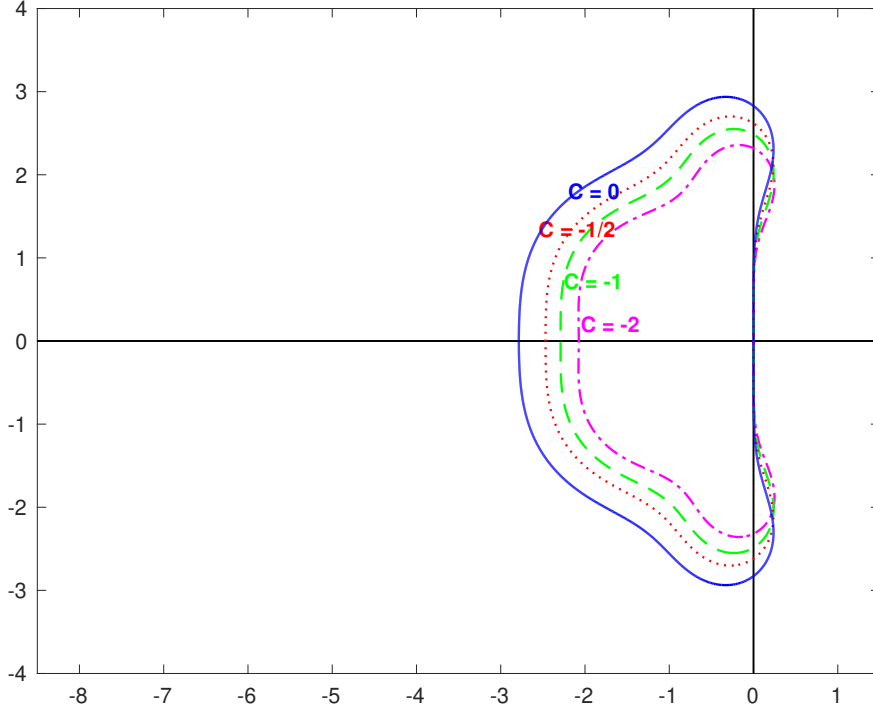


Figure 3.1: Curves of $|f(z, C)| = 1$ with $C = -2, -1, -\frac{1}{2}, 0$.

Remark 3.1. The two-stage fourth-order time discretizations (2.2) may be easily extended to the following system

$$\mathbf{u}'(t) = \mathbf{L}(t, \mathbf{u}), \quad t \in [0, T], \quad \mathbf{u} \in \mathbb{R}^m,$$

subject to $\mathbf{u}(0) = \mathbf{u}_0$, by choosing $\beta = \frac{2}{3}$ and $\boldsymbol{\alpha} = \frac{1}{3}\mathbf{I}_m + \frac{C\tau^3}{60}(\nabla_{\mathbf{u}}\mathbf{L})^3$, where \mathbf{I}_m is an identity matrix of $m \times m$.

3.1. Interval of absolute stability

This subsection discusses the interval of the absolute stability of the two-stage fourth-order time discretizations (2.2) for the case of $z = \tau\lambda \leq 0$ theoretically. Using the definition

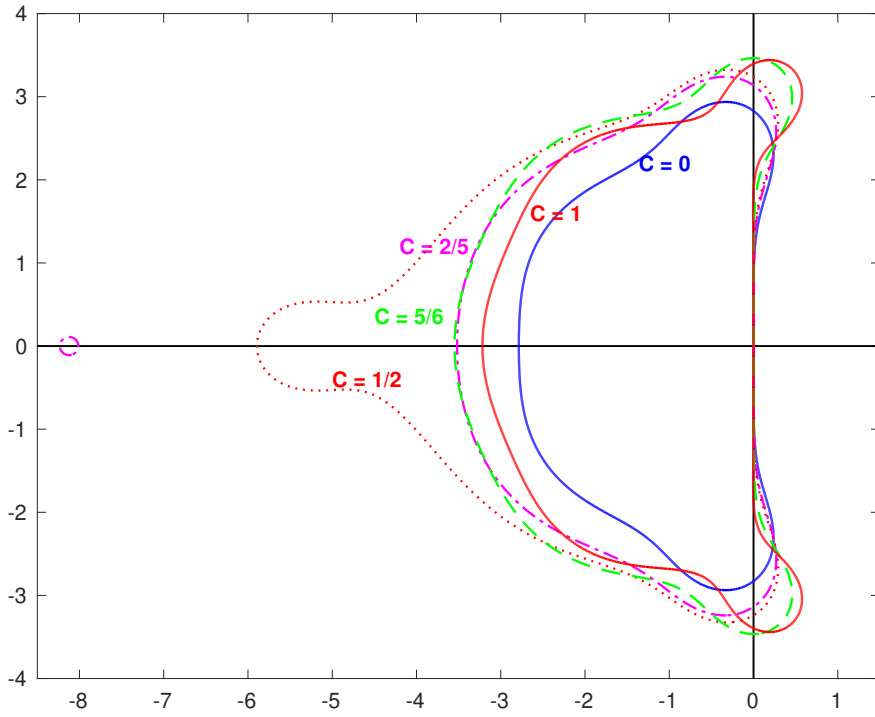


Figure 3.2: Curves of $|f(z, C)| = 1$ with $C = 0, \frac{2}{5}, \frac{1}{2}, \frac{5}{6}, 1$.

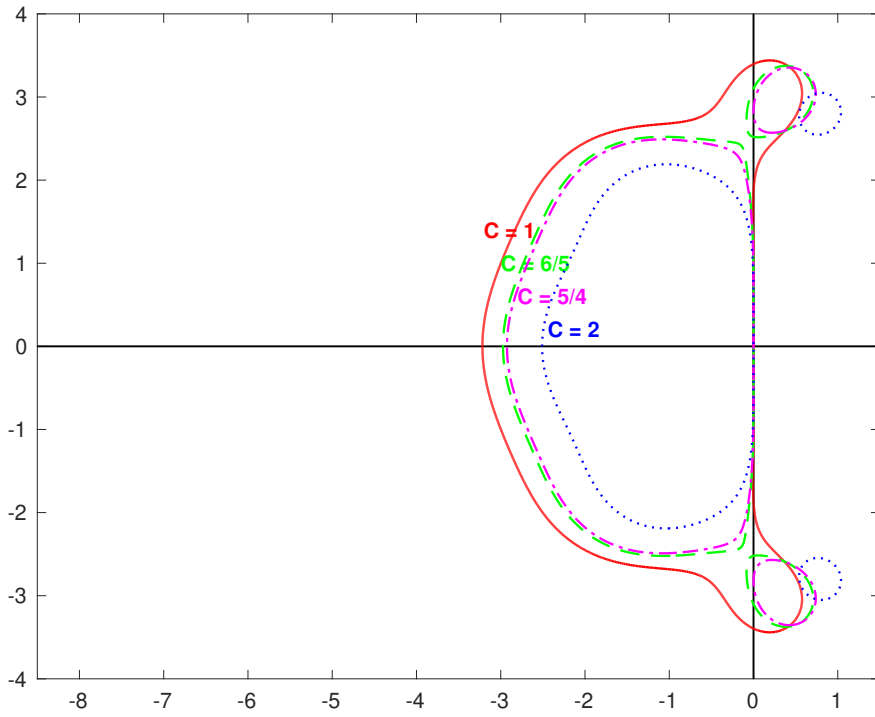


Figure 3.3: Curves of $|f(z, C)| = 1$ with $C = 1, \frac{6}{5}, \frac{5}{4}, 2$.

of $f(z, C)$ and its first-order partial derivative

$$f_z(z, C) = 1 + z + \frac{1}{2}z^2 + \frac{1}{6}z^3 + \frac{C}{24}z^4, \quad (3.4)$$

defines

$$g(z) := f(z, C) - \frac{z}{5}f_z(z, C) = 1 + \frac{4}{5}z + \frac{3}{10}z^2 + \frac{1}{15}z^3 + \frac{1}{120}z^4.$$

Lemma 3.1. The function $g(z)$ satisfies

$$g(z) > 0, \quad \text{for all } z \leq 0.$$

Proof By using the definition of $g(z)$, the derivatives of $g(z)$ are easily given as

$$g_z(z) = \frac{4}{5} + \frac{3}{5}z + \frac{1}{5}z^2 + \frac{1}{30}z^3, \quad g_{zz}(z) = \frac{3}{5} + \frac{2}{5}z + \frac{1}{10}z^2 = \frac{(z+2)^2}{10} + \frac{1}{5}.$$

Because $g_z(-\infty) = -\infty < 0$, $g_z(0) = \frac{4}{5} > 0$, and $g_{zz}(z) > 0$, $g_z(z)$ has a unique negative root, denoted by $z_{g_z}^*$, which is the minimum point of $g(z)$ in $(-\infty, 0)$, that is, $g(z) \geq g(z_{g_z}^*)$ for all $z \leq 0$. Since

$$g(z) - \left(\frac{z}{4} + \frac{1}{2}\right)g_z(z) = \frac{3}{5} + \frac{3}{10}z + \frac{1}{20}z^2 = \frac{(z+3)^2}{20} + \frac{3}{20} > 0,$$

one gets $g(z_{g_z}^*) > 0$. Combining them completes the proof. \square

Using Lemma 3.1 yields the following conclusion.

Lemma 3.2. The local minimum and maximum of $f(z, C)$ in $(-\infty, 0)$ are positive.

Proof If using $z_{f_z}^* \in (-\infty, 0)$ to denote the negative root of $f_z(z, C)$, then one has

$$f(z_{f_z}^*, C) = f(z_{f_z}^*, C) - \frac{z_{f_z}^*}{5}f_z(z_{f_z}^*, C) = g(z_{f_z}^*) > 0.$$

The proof is completed. \square

In the following, we discuss the interval of the absolute stability with the help of Lemma 3.2. Figure 3.4 shows the profiles of $f(z, C)$ with several different C in $z \in (-\infty, 0)$, which can help us understand the discussion.

Case 1: $C \in (-\infty, 0]$. From (3.4), one has

$$f_{zz}(z, C) = 1 + z + \frac{1}{2}z^2 + \frac{C}{6}z^3, \quad (3.5)$$

thus it holds that

$$f_{zz}(z, C) \geq 1 + z + \frac{1}{2}z^2 = \frac{(z+1)^2}{2} + \frac{1}{2} > 0.$$

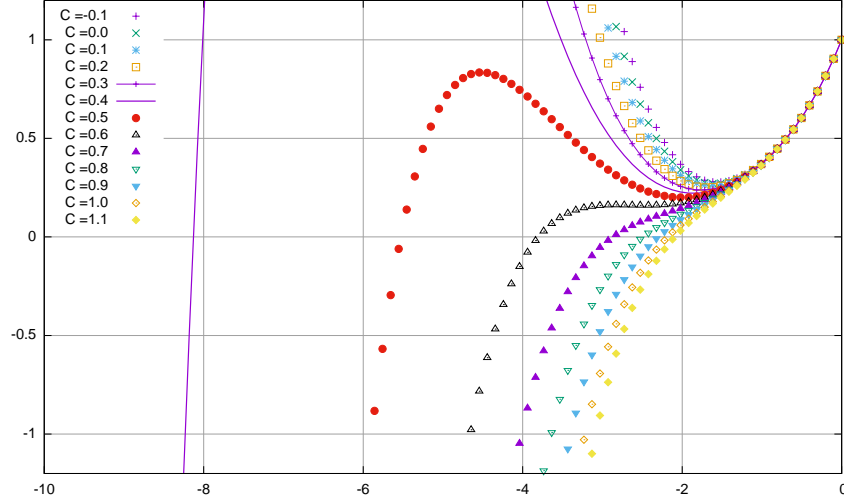


Figure 3.4: The profiles of $f(z, C)$.

It implies that $f(z, C)$ is strictly convex for $z < 0$. Combining $f_{zz}(z, C) > 0$ with $f_z(-\infty, C) = -\infty$ and $f_z(0, C) = 1$ gives that $f_z(z, C)$ has a unique negative root, denoted by $z_{f_z}^*$, which is the minimum point of $f(z, C)$. Using Lemma 3.2 gives

$$0 < f(z_{f_z}^*, C) < f(0, C) = 1.$$

The readers are referred to Figure 3.4. In this case, for each $C \in (-\infty, 0]$, the profile of $f(z, C)$ is similar to that of $f(z, 0)$, and the absolute stability interval $I(C)$ can be expressed as $[z^*(C), 0]$, where $z^*(C)$ is the negative solution of $f(z, C) = 1$. With the help of the fact that $f_C(z, C) = \frac{z^5}{120} < 0$ for $z < 0$, we can conclude that $z^*(C)$ is strictly monotonically increasing in $C \in (-\infty, 0]$.

Case 2: $C \in (0, C_1)$. Here

$$C_1 := \frac{-24 - 24z_1 - 12(z_1)^2 - 4(z_1)^3}{(z_1)^4}, \quad z_1 = -\frac{2(64 + 9\sqrt{67})^{1/3}}{3} + \frac{22}{3(64 + 9\sqrt{67})^{1/3}} - \frac{8}{3},$$

satisfying

$$f_z(z_1, C_1) = 0, \quad f(z_1, C_1) = 1.$$

Some computations can show

$$z_1 \in (-4.689, -4.688), \quad C_1 \in (0.490, 0.491).$$

From (3.5), one has

$$f_{zzz}(z, C) = 1 + z + \frac{C}{2}z^2,$$

and $f_{zzz}(z, C)$ has two real roots, denoted by $z_{f_{zzz},1}^*(C)$ and $z_{f_{zzz},2}^*(C)$ with $z_{f_{zzz},1}^*(C) < z_{f_{zzz},2}^*(C) < 0$. Since

$$f_{zz}(z, C) - \frac{z}{3}f_{zzz}(z, C) = 1 + \frac{2}{3}z + \frac{1}{6}z^2 = \frac{(z+2)^2}{6} + \frac{1}{3} > 0,$$

the local minimum of $f_{zz}(z, C)$ satisfies $f_{zz}(z_{f_{zzz},2}^*(C), C) > 0$. Combining it with $f_{zz}(-\infty, C) = -\infty$ yields that $f_{zz}(z, C)$ has only one root in $(-\infty, 0)$, denoted by $z_{f_{zz}}^*(C)$, which implies that $f_z(z, C)$ is monotonically decreasing in $(-\infty, z_{f_{zz}}^*(C))$ and monotonically increasing in $(z_{f_{zz}}^*(C), 0)$. From Remark 3.2 in the following, one has

$$f_z(z_{f_{zz}}^*(C), C) < 0, \tag{3.6}$$

which means that $f_z(z, C)$ has two negative roots, denoted by $z_{f_z,1}^*(C)$ and $z_{f_z,2}^*(C)$ with $z_{f_z,1}^*(C) < z_{f_z,2}^*(C)$. It is worth noting that that in fact z_1 is a maximum point of $f(z, C_1)$, because of $f(z_{f_z,2}^*(C_1), C_1) < f(0, C_1) = 1$.

On the one hand, one has

$$0 < f(z_{f_z,2}^*(C), C) < f(0, C) = 1.$$

On the other hand, together with $f_C(z, C) = \frac{z^5}{120} < 0$ for $z < 0$, one has

$$f(z_{f_z,1}^*(C_1), C) > f(z_{f_z,1}^*(C_1), C_1) = f(z_1, C_1) = 1.$$

In this case, the profile of $f(z, C)$ is similar to that of $f(z, 0.4)$ as shown in Figure 3.4, and the stability interval $I(C)$ can be expressed as $[z^{*,1}(C), z^{*,2}(C)] \cup [z^{*,3}(C), 0]$, where $z^{*,2}(C), z^{*,3}(C), (z^{*,2}(C) < z^{*,3}(C))$ are the negative solutions of $f(z, C) = 1$ and $z^{*,1}(C)$ is the negative solution of $f(z, C) = -1$.

Case 3: $C \in [C_1, C_2)$. Here

$$C_2 := \frac{-6 - 6z_2 - 3(z_2)^2}{(z_2)^3}, \quad z_2 = -(2 + 2\sqrt{3})^{1/3} + \frac{2}{(2 + 2\sqrt{3})^{1/3}} - 2,$$

satisfying

$$f_z(z_2, C_2) = 0, \quad f_{zz}(z_2, C_2) = 0.$$

Similarly, by some computations, one can show

$$z_2 \in (-2.626, -2.625), \quad C_2 \in (0.603, 0.604).$$

- If $C \in [C_1, 0.5)$, then the same analysis for $C \in (0, C_1)$ can give that $f_z(z, C)$ has two negative roots, denoted by $z_{f_z,1}^*(C)$ and $z_{f_z,2}^*(C)$ with $z_{f_z,1}^*(C) < z_{f_z,2}^*(C)$.
- If $C \in [0.5, C_2)$, then $f_{zzz}(z, C) \geq 0$ for any $z \in \mathbb{R}$. It means that $f_{zz}(z, C)$ is monotonically increasing in $(-\infty, 0)$. Combining it with $f_{zz}(-\infty, C) = -\infty$ and $f_{zz}(0, C) = 1$ gives that $f_{zz}(z, C)$ has a unique root in $(-\infty, 0)$, denoted by $z_{f_{zz}}^*(C) < 0$, such that $f_z(z, C)$ is monotonically decreasing in $(-\infty, z_{f_{zz}}^*(C))$ and monotonically increasing in $(z_{f_{zz}}^*(C), 0)$. Combining those with

$$f_z(-\infty, C) = +\infty, \quad f_z(0, C) = 1,$$

and

$$f_z(z_{f_{zz}}^*(C), C) \leq f_z(z_{f_{zz}}^*(C_2), C) < f_z(z_{f_{zz}}^*(C_2), C_2) = f_z(z_2, C_2) = 0,$$

yields that $f_z(z, C)$ has two negative roots in $(-\infty, 0)$, denoted by $z_{f_z,1}^*(C)$ and $z_{f_z,2}^*(C)$ with $z_{f_z,1}^*(C) < z_{f_z,2}^*(C)$.

Hence, $z_{f_z,1}^*(C)$ is the local maximum point of $f(z, C)$ and $z_{f_z,2}^*(C)$ is the local minimum point of $f(z, C)$. Together with Lemma 3.2 and the definition of C_1 , one can finally obtain

$$0 < f(z_{f_z,2}^*(C), C) < f(z_{f_z,1}^*(C), C) \leq f(z_{f_z,1}^*(C), C_1) \leq 1.$$

Therefore, in this case, the profile of $f(z, C)$ is similar to $f(z, 0.5)$ as shown in Figure 3.4, and the stability interval $I(C)$ can be expressed as $[z^*(C), 0]$, where $z^*(C)$ is the negative solution of $f(z, C) = -1$, and $I(C)$ is strictly monotonically decreasing in $[C_1, C_2)$.

Case 4: $C \in [C_2, \infty)$. Using the same analysis as that for $C \in [0.5, C_2)$ can give that $f_{zz}(z, C)$ has a unique root in $(-\infty, 0)$, denoted by $z_{f_{zz}}^*(C)$, and $f_z(z, C)$ is monotonically decreasing in $(-\infty, z_{f_{zz}}^*(C))$ and monotonically increasing in $(z_{f_{zz}}^*(C), 0)$. With the definition of C_2 , one has

$$f_z(z_{f_{zz}}^*(C), C) \geq f_z(z_{f_{zz}}^*(C), C_2) \geq f_z(z_{f_{zz}}^*(C_2), C_2) = f_z(z_2, C_2) = 0,$$

which implies that the function $f(z, C)$ is monotonically increasing in $(-\infty, 0)$. Therefore, in this case, the profile of $f(z, C)$ is similar to $f(z, 1)$ shown in Figure 3.4, and the stability interval $I(C)$ can be expressed as $[z^*(C), 0]$, where $z^*(C)$ is the negative solution of $f(z, C) = -1$, and $I(C)$ strictly monotonically decreases in $[C_2, +\infty)$.

Remark 3.2. Let us verify the inequality (3.6). It may be proved by contradiction. Assume that $f_z(z_{f_{zz}}^*(C), C) \leq 0$, which implies that the function $f(z, C)$ is monotonically increasing. Some calculations give

$$f(-2, C) = \frac{1}{3} - \frac{4}{15}C, \quad f(-4, C) = 5 - \frac{128}{15}C.$$

Then, one has

$$f(-4, C) - f(-2, C) = \frac{14}{3} - \frac{124}{15}C < 0,$$

which is in contradiction with $C \in (0, 0.5)$.

Remark 3.3. If using z_0^* , $z_{0.5}^*$ and z_1^* to denote the solutions of $f(z, 0) = 1$, $f(z, 0.5) = -1$ and $f(z, 1) = -1$, respectively, then the intervals of the absolute stability of the general two-stage fourth-order time discretizations with $C = 0, 0.5, 1$ are

$$I(0) = [z_0^*, 0], \quad I(0.5) = [z_{0.5}^*, 0], \quad I(1) = [z_1^*, 0],$$

respectively, where z_0^* , $z_{0.5}^*$ and z_1^* satisfy

$$z_0^* \in (-2.786, -2.785), \quad z_{0.5}^* \in (-5.894, -5.893), \quad z_1^* \in (-3.218, -3.217).$$

3.2. Intersection between imaginary axis and stability region

This subsection discusses the intersection between the imaginary axis and the absolute stability region, denoted by $I_{im}(C)$. Let $z = i\zeta$ with $\zeta \in \mathbb{R}$, $i^2 = -1$. Then one has

$$f(i\zeta, C) = 1 - \frac{1}{2}\zeta^2 + \frac{1}{24}\zeta^4 + i \cdot \zeta \left(1 - \frac{1}{6}\zeta^2 + \frac{C}{120}\zeta^4\right),$$

and the value $|f(i\zeta, C)|^2$ can be calculated by

$$\begin{aligned} |f(i\zeta, C)|^2 &= \left(1 - \frac{1}{2}\eta + \frac{1}{24}\eta^2\right)^2 + \eta \left(1 - \frac{1}{6}\eta + \frac{C}{120}\eta^2\right)^2 \\ &= 1 - \frac{\eta^3}{72} + \frac{\eta^4}{576} + \frac{C\eta^3(C\eta^2 - 40\eta + 240)}{14400}, \end{aligned}$$

where $\eta = \zeta^2 \geq 0$. The absolute stability requires that $\eta = 0$ or

$$-\frac{1}{72} + \frac{\eta}{576} + \frac{C(C\eta^2 - 40\eta + 240)}{14400} \leq 0, \quad \text{for } \eta \geq 0. \quad (3.7)$$

If defining

$$g(\eta, C) := C^2\eta^2 + 5(5 - 8C)\eta + 40(6C - 5),$$

then (3.7) is equivalent to $g(\eta, C) \leq 0$ for $\eta \geq 0$. In the following, we discuss its solution.

By some tedious manipulations, we can yield the conditions for (3.7).

- If $C = 0$, then the absolute stability requires $0 \leq \eta \leq 8$, equivalently, $\zeta \in [-2\sqrt{2}, 2\sqrt{2}]$.
- If $C \neq 0$, then calculate the discriminant of the quadratic equation $g(\eta, C) = 0$ by

$$\Delta = (25 - 40C)^2 - 4C^2(240C - 200) = 5(5 - 4C) \cdot (48C^2 - 60C + 25).$$

Because $48C^2 - 60C + 25 > 0$ for all $C \in \mathbb{R}$, the sign of Δ is determined by $5 - 4C$.

- If $C > \frac{5}{4}$, then $\Delta < 0$ and the equation $g(\eta, C) \leq 0$ for $\eta \geq 0$ has no real solution, thus one has

$$|f(i\zeta, C)| \leq 1 \quad \text{if and only if} \quad \zeta = 0.$$

- If $C = \frac{5}{4}$, then $\Delta = 0$ and the equation $g(\eta, C) = 0$ for $\eta \geq 0$ has a unique solution $\eta = 8$, so that

$$|f(i\zeta, C)| \leq 1, \quad \text{if and only if} \quad \zeta = \pm 2\sqrt{2}, 0.$$

- If $C < \frac{5}{4}$, then $\Delta > 0$ and the equation $g(\eta, C) = 0$ for $\eta \geq 0$ has two different real solutions

$$\eta_- = \frac{-(25 - 40C) - \sqrt{\Delta}}{2C^2}, \quad \eta_+ = \frac{-(25 - 40C) + \sqrt{\Delta}}{2C^2}.$$

According to the sign of $g(0, C)$, our discussion is divided into three cases.

- * If $C < \frac{5}{6}$, then $g(0, C) < 0$, thus $\eta_+ > 0$ and $\eta_- < 0$, so that the inequality $g(\eta, C) \leq 0$ for $\eta \geq 0$ requires $0 \leq \eta \leq \eta_+$. That is to say,

$$|f(i\zeta, C)| \leq 1, \quad \text{if and only if} \quad \zeta \in [-\sqrt{\eta_+}, \sqrt{\eta_+}].$$

- * If $C = \frac{5}{6}$, then $\eta_+ > 0$, $\eta_- = 0$, and the inequality $g(\eta, C) \leq 0$ for $\eta \geq 0$ requires gives $0 \leq \eta \leq \eta_+$. That is to say,

$$|f(i\zeta, C)| \leq 1, \quad \text{if and only if} \quad \zeta \in [-\sqrt{\eta_+}, \sqrt{\eta_+}]. \quad (3.8)$$

- * If $C \in (\frac{5}{6}, \frac{5}{4})$, then $\eta_+ > 0$, $\eta_- > 0$, and thus the inequality $g(\eta, C) \leq 0$ for $\eta \geq 0$ requires $\eta_- \leq \eta \leq \eta_+$. That is to say,

$$|f(i\zeta, C)| \leq 1, \quad \text{if and only if} \quad \zeta \in [-\sqrt{\eta_+}, -\sqrt{\eta_-}] \cup [\sqrt{\eta_-}, \sqrt{\eta_+}] \cup 0.$$

In all, the interval $I_{im}(C)$ can be summed up as follows

$$I_{im}(C) = \begin{cases} [-\sqrt{\eta_+}, \sqrt{\eta_+}], & \text{if } C < 0; \\ [-2\sqrt{2}, 2\sqrt{2}], & \text{if } C = 0; \\ [-\sqrt{\eta_+}, \sqrt{\eta_+}], & \text{if } C \in (0, \frac{5}{6}); \\ [-\sqrt{\eta_+}, -\sqrt{\eta_-}] \cup [\sqrt{\eta_-}, \sqrt{\eta_+}] \cup \{0\}, & \text{if } C \in (\frac{5}{6}, \frac{5}{4}); \\ \{-2\sqrt{2}, 2\sqrt{2}, 0\}, & \text{if } C = \frac{5}{4}; \\ \{0\}, & \text{if } C \in (\frac{5}{4}, \infty). \end{cases} \quad (3.9)$$

When $C = 0, 0.5, 1$, the intersections $I_{im}(C)$ between the imaginary axis and the absolute stability regions are explicitly and respectively given by

$$I_{im}(0) = [-2\sqrt{2}, 2\sqrt{2}], \quad I_{im}(0.5) = \left[-\sqrt{2(\sqrt{105} - 5)}, \sqrt{2(\sqrt{105} - 5)} \right],$$

$$I_{im}(1) = \left[-\sqrt{\frac{15 + \sqrt{65}}{2}}, -\sqrt{\frac{15 - \sqrt{65}}{2}} \right] \cup \left[\sqrt{\frac{15 - \sqrt{65}}{2}}, \sqrt{\frac{15 + \sqrt{65}}{2}} \right] \cup 0.$$

Remark 3.4. For the case of $C < \frac{5}{6}$ and $C \neq 0$, see (3.9), one can know that $I_{im}(C)$ depends on the positive root η_+ of $g(\eta, C)$. On the other hand, thanks to $g(8, C) = 16C(4C - 5)$, $g(8, C) > 0$ if $C < 0$ and $g(8, C) < 0$ for $C \in (0, \frac{5}{6})$. Hence, $I_{im}(C)$ satisfies

$$\begin{cases} I_{im}(C) \subsetneq I_{im}(0), & \text{if } C < 0; \\ I_{im}(C) \supsetneq I_{im}(0), & \text{if } C \in (0, \frac{5}{6}). \end{cases}$$

For $C \in (\frac{5}{6}, \frac{5}{4})$, see (3.9), $I_{im}(C)$ depends on the roots η_{\pm} of $g(\eta, C)$. Because $\partial_C g(\eta, C) = 2C\eta^2 - 40\eta + 240 > \frac{5}{3}\eta^2 - 40\eta + 240 \geq 0$, the set $\{\eta \mid g(\eta, C) \leq 0, \eta \geq 0\}$ decreases as C increases, and thus one can get

$$\begin{cases} I_{im}(C) \subsetneq I_{im}(1), & \text{if } C \in (1, \frac{5}{4}); \\ I_{im}(C) \supsetneq I_{im}(1), & \text{if } C \in (\frac{5}{6}, 1). \end{cases}$$

For $I_{im}(C)$, the choice of C in $[0, 1]$ is better than $C < 0$ and $C > 1$.

4. Numerical results

This section conducts several numerical experiments to demonstrate the performance and the above analyses of the general two-stage fourth-order time discretizations (2.2) with (3.1),

in comparison with the following four-stage fourth-order Runge-Kutta method (abbreviated by RK4)

$$\begin{cases} u^{(1)} = u^n + \frac{1}{2}\tau L(t^n, u^n), \\ u^{(2)} = u^n + \frac{1}{2}\tau L(t^n + \frac{1}{2}\tau, u^{(1)}), \\ u^{(3)} = u^n + \tau L(t^n + \frac{1}{2}\tau, u^{(2)}), \\ u^{n+1} = \frac{1}{3} \left[u^{(1)} + 2u^{(2)} + u^{(3)} - u^n + \frac{1}{2}\tau L(t^n + \tau, u^{(3)}) \right]. \end{cases}$$

The following will only show the numerical results obtained with $C = 0, 0.5, 1$, which are better than the choice of $C < 0$ or $C > 1$ as shown in Section 3. The diagrams will be drawn with symbols “o”, “+” and “Δ”, and “□” for the two-stage fourth-order time discretizations (2.2) with (3.1) and $C = 0, 0.5, 1$, and RK4, respectively.

4.1. Scalar case

This subsection will solve several first-order ordinary differential equations by using the two-stage high-order methods (2.2) with $\alpha = \frac{1}{3} + \frac{C}{60}(L_u\tau)^3$, $\beta = \frac{2}{3}$ or $\alpha = \frac{1}{3}$, $\beta = \frac{2}{3} + \frac{C}{60}(L_u\tau)^3$. The constant C is taken as $C = 0, 0.5, 1$, respectively, and the relative error

$$err(u) = \frac{|u(T) - u_\tau(T)|}{|u(T)|},$$

is estimated, where $u(T)$ and $u_\tau(T)$ are the exact and numerical solutions at $t = T$, respectively.

Example 4.1. Consider the initial value problem

$$u'(t) = -u, \quad t \geq 0; \quad u(0) = 1, \quad (4.1)$$

whose exact solution is $u(t) = \exp(-t)$.

Table 4.1 gives the relative errors and convergence rates at $t = 4$ obtained by the method (2.2) with $\alpha = \frac{1}{3} + \frac{C}{60}(L_u\tau)^3$, $\beta = \frac{2}{3}$, where the reference step-sizes τ_0 are given by the intervals of the absolute stability in Remark 3.3. The result clearly shows that for the model problem (4.1) the proposed method with $C = 0$ or 0.5 is fourth-order accurate, and (2.2) with $C = 1$ is fifth-order accurate. It is consistent with the previous theoretical analysis. In this test, the numerical results obtained by $\alpha = \frac{1}{3}$, $\beta = \frac{2}{3} + \frac{C}{60}(L_u\tau)^3$ are the same as those in Table 4.1, so they are not presented here to avoid repetition.

Table 4.1: Example 4.1: The relative errors and convergence rates of the general two-stage fourth-order time discretization with $\alpha = \frac{1}{3} + \frac{C}{60}(L_u\tau)^3$, $\beta = \frac{2}{3}$ and reference step-size τ_0 .

τ	$C = 0, \tau_0 = 2.7$		$C = 0.5, \tau_0 = 5.8$		$C = 1, \tau_0 = 3.2$	
	error	order	error	order	error	order
τ_0	1.3291e+01	-	3.9039e+01	-	2.4742e+01	-
$\tau_0/2$	3.6366e-01	5.1917	5.1269e+00	2.9287	1.7886e-01	7.1120
$\tau_0/4$	1.1691e-02	4.9591	1.5732e-01	5.0263	3.6257e-03	5.6244
$\tau_0/8$	5.5332e-04	4.4011	6.7895e-03	4.5343	8.0248e-05	5.4976
$\tau_0/16$	3.0414e-05	4.1853	3.6496e-04	4.2175	2.1109e-06	5.2486
$\tau_0/32$	1.7974e-06	4.0807	2.0228e-05	4.1733	6.0532e-08	5.1240

Example 4.2. Solve the initial value problem

$$u'(t) = L(t, u) = \lambda(u - \cos t) - \sin t, \quad t \geq 0, \quad \lambda = -2100; \quad u(0) = 1,$$

whose exact solution is $u(t) = \cos t$. In this case, $L_u = \lambda$ is constant so that the step-size can also be taken as a constant following the interval of the absolute stability in Remark 3.3. Figure 4.1 displays the relative errors. Those results show that the errors tend to infinity as time increases if the step-size τ is chosen as the smallest such that $\lambda\tau \notin I(C)$, but if the step-size τ is taken as the biggest such that $\lambda\tau \in I(C)$, then both the present method (2.2) and RK4 are stable and the errors of (2.2) are smaller than those of RK4. Moreover, the biggest step-size for the stability of (2.2) with $C = 0.5$ is almost twice those of (2.2) with $C = 0$ or 1 and RK4.

Example 4.3. Consider the initial value problem of a nonlinear differential equation

$$u'(t) = \mu_1(u - \cos(t)) + \mu_2(u^2 - \cos^2(t)) - \sin(t), \quad t \geq 0; \quad u(0) = 1, \quad (4.2)$$

whose exact solution $u(t) = \cos(t)$. In this case, $L_u = \mu_1 + 2\mu_2u$ is not a constant so that the biggest step-size for the stability is no longer constant.

Our calculations take $\mu_1 = -2100$ and $\mu_2 = 10$. Figure 4.2 plots the relative errors by our methods and RK4 with different τ . The results show that the errors of the present method and RK4 grow over time t if the step-size τ is chosen as the smallest such that $L_u\tau \notin I(C)$, but if τ is taken as the biggest such that $L_u\tau \in I(C)$, those time discretizations are stable and the errors of the proposed methods are smaller than those of RK4.

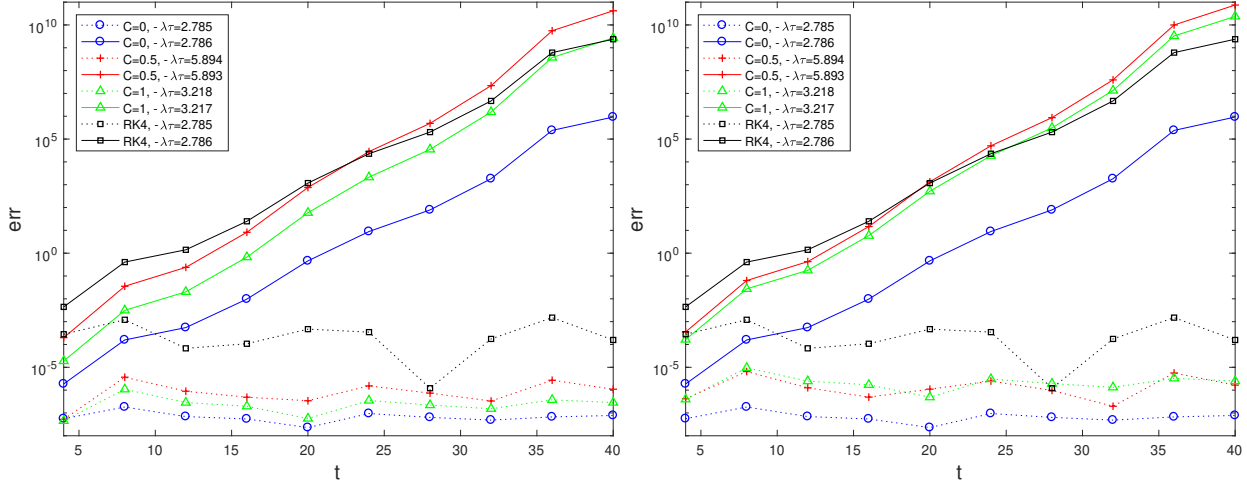


Figure 4.1: Example 4.2: Relative errors obtained by the general two-stage fourth-order time discretizations and RK4 with different step-sizes τ . Left: $\alpha = \frac{1}{3} + \frac{C}{60}(\lambda\tau)^3$, $\beta = \frac{2}{3}$; right: $\alpha = \frac{2}{3}$, $\beta = \frac{1}{3} + \frac{C}{60}(\lambda\tau)^3$.

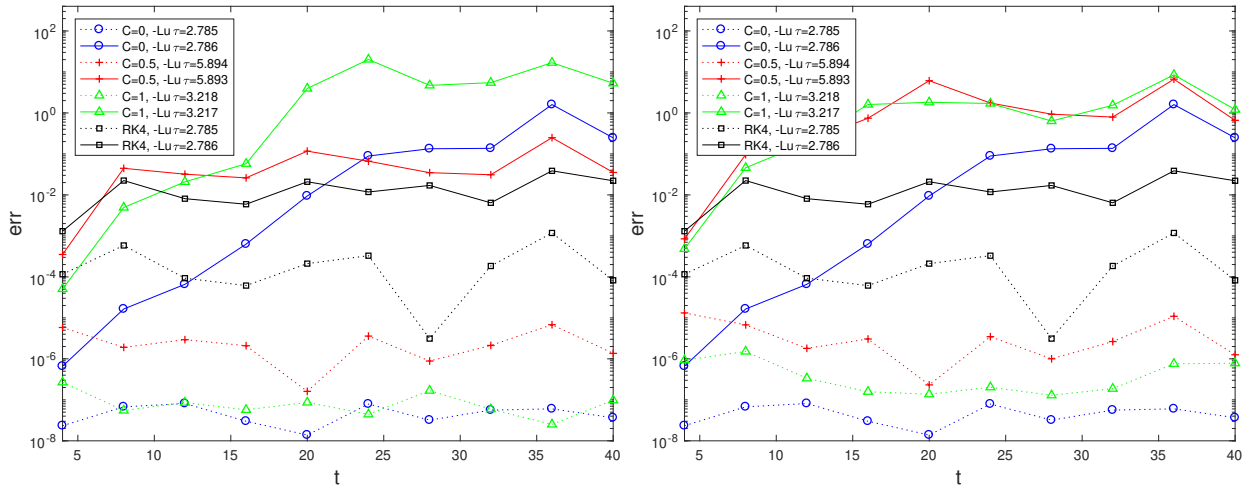


Figure 4.2: Example 4.3: Relative errors obtained by the general two-stage fourth-order time discretizations and RK4 with different step-sizes τ . Left: $\alpha = \frac{1}{3} + \frac{C}{60}(L_u\tau)^3$, $\beta = \frac{2}{3}$; right: $\alpha = \frac{2}{3}$, $\beta = \frac{1}{3} + \frac{C}{60}(L_u\tau)^3$.

4.2. System case

This subsection will solve several system of ordinary differential equations by using the two-stage high-order methods (2.2) with $\alpha = \frac{1}{3}\mathbf{I} + \frac{C\tau^3}{60}(\nabla_{\mathbf{u}}\mathbf{L})^3$, $\beta = \frac{2}{3}$, and $C = 0, 0.5, 1$.

Example 4.4. *This example considers the second-order ODE $mq''(t) = -kq(t) - cq'(t)$, describing the motion of a spring oscillator. By introducing $p(t) = mq'(t)$, it can be converted to the following system*

$$\mathbf{u}' = \mathbf{L}(\mathbf{u}), \quad \mathbf{u} = \begin{pmatrix} p \\ q \end{pmatrix}, \quad \mathbf{L}(\mathbf{u}) = \begin{pmatrix} -\frac{c}{m} & -k \\ \frac{1}{m} & 0 \end{pmatrix} \mathbf{u}.$$

Our calculations take the parameters as $m = 1, c = 1001, k = 1000$ and the initial data as $p(0) = -1, q(0) = 1$. Some manipulations show the eigenvalues $\lambda_1 = -1000, \lambda_2 = -1$ of $\mathbf{L}\mathbf{u}(\mathbf{u})$ and the exact solution $(p, q) = e^{-t}(-1, 1)$.

Figure 4.3 plots the relative errors by our methods and RK4 with different step-sizes τ . The results show that the errors of our methods and RK4 increase to infinity over time if τ is chosen as the smallest outside the interval of absolute stability, but if τ is chosen as the biggest available step-sizes inside the interval of absolute stability, our methods with $C = 0, 1$ and RK4 are stable. Nevertheless, the errors of p obtained by our method with $C = 0.5$ grow over time. Table 4.2 lists the steps and errors by our methods with $C = 0.5, 1$ and $-\lambda_1\tau = 2.785$. It can be seen that our methods are stable now, and the errors are the same size as those with $C = 0$.

Example 4.5. *The last example solves the Lorenz system*

$$\begin{cases} x'(t) = a(y - x), \\ y'(t) = cx - y - xz, \\ z'(t) = xy - bz, \end{cases}$$

where a, b, c are constant. The behavior depends on the parameters a, b, c . If we take $a = 61.8, b = 8/3, c = 28$, the system has three stationary points: $(x_1, y_1, z_1) = (0, 0, 0)$, $(x_2, y_2, z_2) = (6\sqrt{2}, 6\sqrt{2}, 27)$ and $(x_3, y_3, z_3) = (-6\sqrt{2}, -6\sqrt{2}, 27)$, where the stationary point $(0, 0, 0)$ is unstable, while the other two are stable.

Our calculations take the initial data $x(0) = 4, y(0) = 4, z(0) = 8$. Tables 4.3 – 4.6 list the relative errors

$$\text{err}(u) = \frac{|u^{\text{ref}}(T) - u_{\tau}(T)|}{|u^{\text{ref}}(T)|}, \quad u = x, y, z,$$

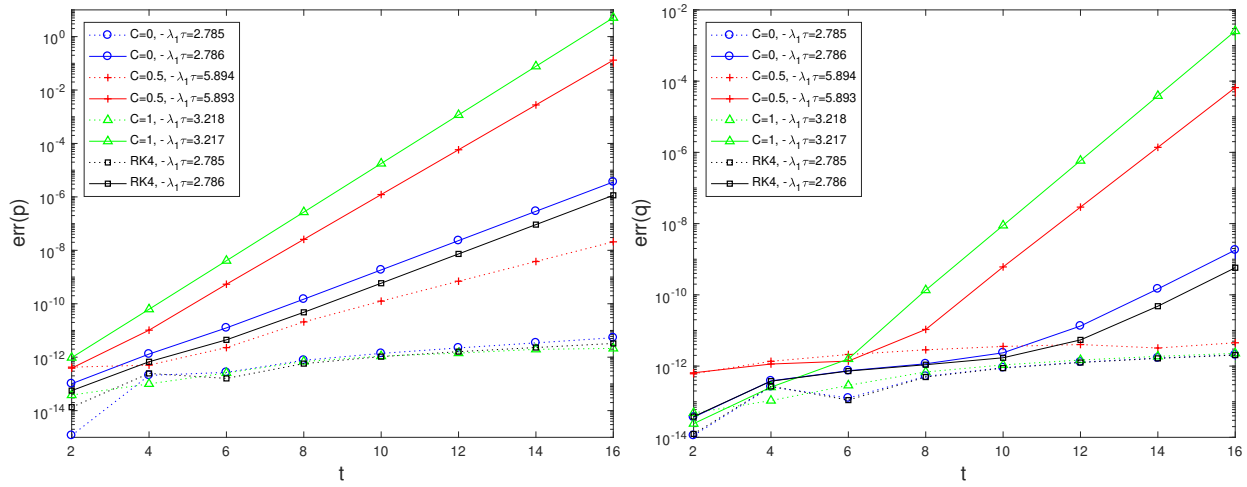


Figure 4.3: Example 4.4: Relative errors obtained by the general two-stage fourth-order time discretizations and RK4 with different step-sizes τ . Left: $err(p)$; right: $err(q)$.

Table 4.2: Example 4.4: The time steps and errors at $t = 2, 4, \dots, 16$ obtained by the general two-stage fourth-order time discretization with $C = 0.5$ or 1 and $-\lambda_1\tau = 2.785$.

t	step	$C = 0.5$		$C = 1$	
		$err(p)$	$err(q)$	$err(p)$	$err(q)$
2	1437	2.571e-14	2.604e-14	5.746e-14	5.746e-14
4	2874	1.938e-13	1.938e-13	1.373e-13	1.376e-13
6	4311	2.325e-13	2.325e-13	3.114e-13	3.113e-13
8	5748	6.518e-13	6.518e-13	7.596e-13	7.591e-13
10	7185	1.072e-12	1.072e-12	1.209e-12	1.209e-12
12	8622	1.492e-12	1.492e-12	1.655e-12	1.655e-12
14	10059	1.909e-12	1.910e-12	2.105e-12	2.105e-12
16	11496	2.327e-12	2.327e-12	2.555e-12	2.555e-12

at $t = 1, 2, \dots, 10$ obtained by our methods and RK4 with different step-sizes τ , where $u^{ref}(T)$ is the reference solution obtained by RK4 with $\tau = 0.001$. Figure 4.4 shows the solutions over time with different C and step-sizes τ . The results show that the method with $C = 0.5$ permits larger step-size than that with $C = 0$ or 1. It is worthy to note that the program of our method with $C = 0$ or 1 will break up if $\tau = 0.0625$.

Table 4.3: Example 4.5: Errors at $t = 1, 2, \dots, 10$ obtained by the general two-stage fourth-order time discretization with $C = 0$.

t	$\tau = 0.04$			$\tau = 0.01$		
	$err(x)$	$err(y)$	$err(z)$	$err(x)$	$err(y)$	$err(z)$
1	6.7015e-02	2.9769e-03	9.9755e-02	2.0257e-05	1.7648e-05	4.4321e-06
2	1.7809e-01	2.0776e-01	4.4027e-02	3.0170e-06	5.8543e-06	7.1119e-06
3	1.8387e-02	5.9763e-03	6.1340e-02	6.5192e-06	4.9609e-06	4.4250e-06
4	4.5944e-02	3.8950e-02	2.0328e-02	6.0860e-06	5.8296e-06	1.0720e-06
5	2.5444e-02	2.5753e-02	1.3452e-03	2.9386e-06	3.2706e-06	5.3503e-07
6	7.0759e-03	8.7117e-03	3.1256e-03	4.1393e-07	7.6983e-07	7.7225e-07
7	6.7926e-04	3.1301e-04	2.2993e-03	5.5782e-07	3.8339e-07	4.4008e-07
8	1.8880e-03	1.5924e-03	8.2682e-04	5.3004e-07	5.0065e-07	1.1080e-07
9	1.0623e-03	1.0787e-03	5.1666e-05	2.3573e-07	2.6121e-07	3.8009e-08
10	2.8804e-04	3.5932e-04	1.3760e-04	3.0994e-08	5.6925e-08	5.6218e-08

5. Conclusion

By introducing variable weights, this paper proposed a class of more general explicit one-step two-stage time discretizations, which are different from the existing methods, such as the Euler methods, Runge-Kutta methods, and multistage multiderivative methods etc. Their absolute stability, the stability interval, and the intersection between the imaginary axis and the absolute stability region were carefully studied. The results showed that the new two-stage time discretizations could be fourth-order accurate conditionally, the absolute stability region of the proposed methods with some special choices of the variable weights could be larger than that of the classical explicit fourth- or fifth-order Runge-Kutta method, and the interval of absolute stability can be almost twice as much as the latter. Several

Table 4.4: Example 4.5: Same as Table 4.3 except for $C = 0.5$.

t	$\tau = 0.0625$			$\tau = 0.01$		
	$err(x)$	$err(y)$	$err(z)$	$err(x)$	$err(y)$	$err(z)$
1	9.3319e-02	3.2845e-02	5.7565e-02	2.0617e-06	3.7958e-06	4.2273e-06
2	9.1353e-02	1.1158e-01	3.7513e-02	4.8728e-06	7.8086e-06	6.0057e-06
3	2.1367e-02	9.4735e-03	3.4155e-02	4.9381e-06	3.3219e-06	4.0089e-06
4	2.7067e-02	2.4241e-02	9.1287e-03	4.6001e-06	4.3271e-06	1.0246e-06
5	1.2676e-02	1.3233e-02	2.5175e-04	2.2045e-06	2.4134e-06	2.9472e-07
6	2.8142e-03	3.7420e-03	1.8532e-03	3.6937e-07	6.0478e-07	5.0476e-07
7	6.7871e-04	2.0339e-04	1.1253e-03	3.2916e-07	2.1215e-07	2.9230e-07
8	9.6442e-04	8.4702e-04	3.4594e-04	3.3149e-07	3.0952e-07	7.7360e-08
9	4.7010e-04	4.8793e-04	1.1421e-06	1.5024e-07	1.6457e-07	1.9940e-08
10	1.0853e-04	1.4200e-04	6.6884e-05	2.2575e-08	3.8093e-08	3.3305e-08

Table 4.5: Example 4.5: Same as Table 4.3 except for $C = 1$.

t	$\tau = 0.04$			$\tau = 0.01$		
	$err(x)$	$err(y)$	$err(z)$	$err(x)$	$err(y)$	$err(z)$
1	1.5361e-03	1.9805e-03	6.4616e-03	1.6156e-05	1.0065e-05	4.0029e-06
2	8.5945e-03	1.3262e-02	7.0901e-03	6.7043e-06	9.7256e-06	4.8799e-06
3	4.9792e-03	3.1234e-03	4.8734e-03	3.3433e-06	1.6740e-06	3.5795e-06
4	4.4063e-03	4.1019e-03	1.1500e-03	3.1021e-06	2.8133e-06	9.7422e-07
5	1.9307e-03	2.0774e-03	1.7791e-04	1.4654e-06	1.5507e-06	5.3838e-08
6	3.4475e-04	5.1191e-04	3.5437e-04	3.2398e-07	4.3844e-07	2.3630e-07
7	1.8519e-04	1.0561e-04	1.9561e-04	9.9956e-08	4.0592e-08	1.4400e-07
8	1.9198e-04	1.7594e-04	5.2216e-05	1.3241e-07	1.1792e-07	4.3785e-08
9	8.5114e-05	9.1504e-05	7.3770e-06	6.4516e-08	6.7691e-08	1.8473e-09
10	1.4865e-05	2.2347e-05	1.5720e-05	1.4119e-08	1.9205e-08	1.0349e-08

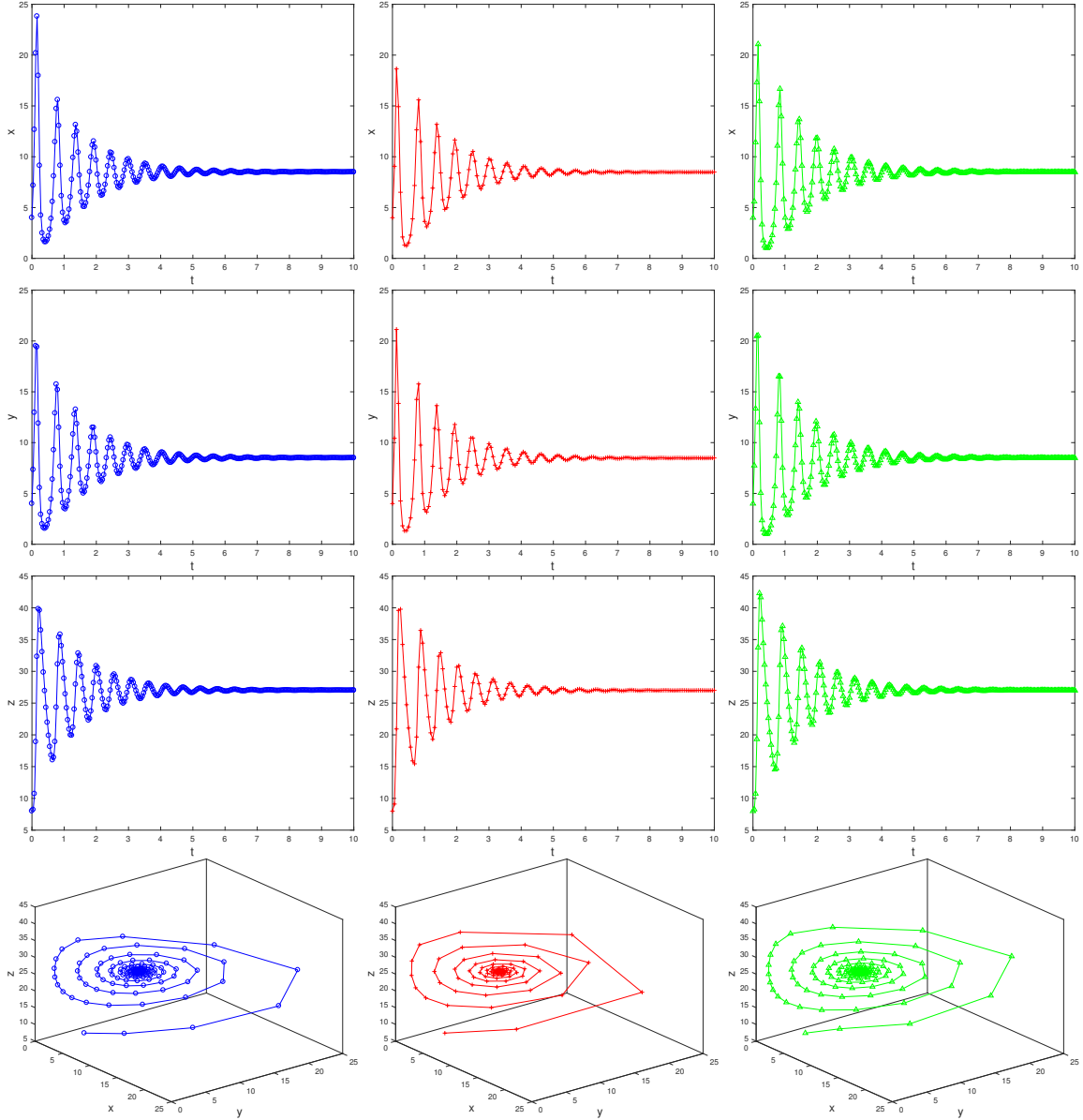


Figure 4.4: Example 4.5: Solutions (From top to bottom: x, y, z and trajectories) obtained by the general two-stage fourth-order time discretizations. Left: $C = 0, \tau = 0.04$; middle: $C = 0.5, \tau = 0.0625$; right: $C = 1, \tau = 0.04$.

Table 4.6: Example 4.5: Same as Table 4.3 except for RK4.

t	$\tau = 0.04$			$\tau = 0.01$		
	$err(x)$	$err(y)$	$err(z)$	$err(x)$	$err(y)$	$err(z)$
1	4.2184e-02	2.3244e-02	2.1487e-02	4.0999e-05	2.2965e-05	8.8756e-06
2	2.1815e-02	3.3483e-02	2.3926e-02	1.0701e-05	1.6094e-05	1.0973e-05
3	1.7573e-02	1.3117e-02	1.3310e-02	8.9941e-06	6.7554e-06	7.6197e-06
4	1.3504e-02	1.2992e-02	2.3494e-03	8.8726e-06	8.4220e-06	1.7920e-06
5	5.1771e-03	5.8316e-03	1.0917e-03	4.1519e-06	4.5617e-06	6.5426e-07
6	4.3010e-04	9.9634e-04	1.2432e-03	6.1669e-07	1.0786e-06	9.9454e-07
7	8.7431e-04	6.4763e-04	5.8343e-04	6.7845e-07	4.5406e-07	5.6068e-07
8	6.6585e-04	6.4333e-04	1.0654e-04	6.4966e-07	6.1090e-07	1.4192e-07
9	2.4192e-04	2.7694e-04	5.9139e-05	2.8740e-07	3.1716e-07	4.3333e-08
10	1.1922e-05	3.9662e-05	6.1925e-05	3.9208e-08	6.9809e-08	6.6129e-08

numerical experiments were carried out to demonstrate the performance and accuracy as well as the stability of the proposed methods. It is interesting to apply the present time discretization to solving the time-dependent partial differential equations.

Acknowledgments

The authors were partially supported by the Special Project on High-performance Computing under the National Key R&D Program (No. 2016YFB0200603), Science Challenge Project (No. TZ2016002), the Sino-German Cooperation Group Project (No. GZ 1465), and the National Natural Science Foundation of China (No. 11421101).

References

- [1] R.P.K. Chan and A.Y.J. Tsai. On explicit two-derivative Runge-Kutta methods. *New Astron.*, 53(2): 171–194, 2010.
- [2] E. Hairer, S.P. Nørsett, and G. Wanner. *Solving Ordinary Differential Equations I: Nonstiff Problems, 2nd revised. ed.*, Springer-Verlag, 1993.
- [3] K.H. Kastlunger and G. Wanner. Runge Kutta processes with multiple nodes. *Computing*, 9(1): 9–24, 1972.

- [4] R.J. LeVeque. *Finite Difference Methods for Ordinary and Partial Differential Equations. Steady-State and Time-Dependent Problems*. Society for Industrial and Applied Mathematics, 2007.
- [5] J.Q. Li and Z.F. Du. A two-stage fourth order time-accurate discretization for Lax-Wendroff type flow solvers. I. hyperbolic conservation laws. *SIAM J. Sci. Comput.*, 38(5): A3046–A3069, 2016.
- [6] A.Y.J. Tsai, R.P.K. Chan, and S.X. Wang. Two-derivative Runge-Kutta methods for PDEs using a novel discretization approach. *New Astron.*, 65: 687–703, 2014.
- [7] Y.H. Yuan and H.Z. Tang. Two-stage fourth-order accurate time discretizations for 1D and 2D special relativistic hydrodynamics. *J. Comput. Math.*, 38(5):768-796, 2020.